Activation Rate of Seismicity for Hydraulic Fracture Wells in the Western Canada Sedimentary Basin – An update

Hadi Ghofrani and Gail M. Atkinson, Western University

October 2021

Abstract

The average regional rate of **M**≥2 earthquakes associated with hydraulic fracture (HF) wells is ~0.03 per well for Alberta and 1.4 for northeastern British Columbia (NEBC); the corresponding per well seismicity rates for **M**≥3 (assuming a Gutenberg Richter slope of 1) are ~0.003 and 0.14, respectively. Overall, ~50% of all observed **M**≥2 seismicity in central Alberta, and ~70% in NEBC, appears related in time and space to HF wells. These rates are consistent with those of several previous studies; the consistency across studies that utilized evolving methodologies provides confidence that the results are robust, in the regional average context in which they are intended.

Within each region, the rate of association of seismicity with HF wells varies greatly with formation and age. In Alberta, there is a clear trend to increasing activation potential with depth and age. In NEBC, the trend is less clear, although this may be largely attributed to the lack of HF wells in deeper and older formations.

The conclusions of the study are derived from the use of an objective measure (the W metric) to assess the degree of spatiotemporal association between earthquakes and HF wells. The study builds on previous work (Atkinson et al., 2016; Ghofrani and Atkinson, 2020) by refining the metric used to assess potential association and applying it to improved earthquake catalogues. We explicitly adjust for overcounting of association rates due to false positives, demonstrating that the obtained rates are consistent with expectations based on observed seismicity patterns.

Introduction

The rise of horizontal drilling and associated technologies to enhance oil and gas recovery in tight reservoirs, beginning in 2010, has led to dramatic increases in seismicity rates throughout central North America (Ellsworth, 2013). In the U.S., most of the seismicity has been associated with the disposal of co-produced wastewater (Ellsworth, 2013; Rubinstein and Mahani, 2016), whereas in Canada's western Canada sedimentary basin (WCSB) most of the seismicity has been associated with hydraulic fracturing (Atkinson et al., 2016). The association of seismicity with hydraulic fracturing of horizontal wells (HF wells) in the WCSB has been documented in a series of papers that fall broadly into two categories: (i) detailed studies of prolific event sequences triggered by nearby HF wells (e.g. Schultz et al.,2015a,b; Wang et al., 2020); and (ii) statistical studies taking a broad view of the association between seismicity and HF wells (e.g. Atkinson et al., 2016; Ghofrani and Atkinson, 2016, 2020; Pawley et al., 2016; Chapman, 2021). The former class of studies is aimed at establishing a clear link for specific instances of HF-triggered seismicity and exploring the mechanics of the process. This is critical for development of event discrimination technologies and improved understanding of HF processes (e.g. Schultz et al.,

2020a). By contrast, statistical studies aim to characterize the association and its attributes on a regional scale. This is useful for the assessment or forecasting of seismic hazard from such operations in a more generic context (e.g. Atkinson, 2017; Ghofrani et al., 2020). For more details on these approaches and their findings, the reader is referred to two recent literature review papers (Schultz et al., 2020a; Atkinson et al., 2020), which likewise tend to direct their focus towards issues of process and hazard implications, respectively.

The statistical relationship between HF wells and seismicity on a regional scale in the WCSB has been explored in a series of papers. Atkinson et al. (2016) examined the relationship between oil and gas activities and earthquakes of moment magnitude (**M**)≥3 from 1985-2015. They showed that a dramatic increase in regional seismicity rates began in 2011, tracking a dramatic increase in HF wells that began in 2010. They flagged **M**≥3 events that occurred within 20 km and 90 days of HF wells and evaluated each flagged event to make a subjective judgement of the likelihood for potential association; the potential role of disposal wells was also considered in the assessment. Atkinson et al. (2016) concluded that, as a regional average, approximately 0.2 to 0.4% of HF wells in the WCSB are associated with **M**≥3 seismicity. They also concluded that, from 2010 to 2015, more than half of the **M**≥3 events in the WCSB are associated with HF wells.

Ghofrani and Atkinson (2016) took a slightly different approach to evaluate the relationship between seismicity and HF wells and how it varies spatially over the WCSB. They gridded the WCSB into overlapping cells of 10 km radius and identified all cells in which **M**≥3 earthquakes occurred within 90 days following one or more HF well operations. This allowed an evaluation of the rate of seismicity on a per unit area basis, which is convenient for probabilistic seismic hazard assessment (PSHA) (e.g. Atkinson, 2017). They concluded that the likelihood that HF operations in an area of 10 km radius will be associated with **M**≥3 earthquakes is in the range of ~1% to 3% (at the 95th percentile confidence limit) on average over the WCSB. The proximity to a nearby disposal well increases the likelihood of association, as does proximity to the Swan Hills Formation, a geologic proxy for basement-controlled faults (i.e. see Schultz et al., 2016). The average WCSB results of Ghofrani and Atkinson (2016) for a 10 km cell are consistent with the per-well rates of Atkinson et al. (2016), considering that the average number of HF wells per cell is 8 (i.e. a cellular rate of 1% to 3% is equivalent to a per well rate of 0.1% to 0.4%). In both Atkinson et al. (2016) and Ghofrani and Atkinson (2016), the designation of HF wells as potentially associated was facilitated by subjective judgement, though it was acknowledged that many cases are inherently ambiguous.

Most recently, Ghofrani and Atkinson (2020; GA20) built on the studies of Atkinson et al. (2016) and Ghofrani and Atkinson (2020) by defining a simple objective metric of the spatiotemporal link between HF wells and seismicity. The idea is to replace a subjective assessment with a score reflecting the degree of association, in which HF wells that are closely associated with earthquakes in both time and space receive a high score (maximum of 1), whereas HF wells that are further away in time and space have low likelihood of association (minimum of 0). They began by flagging **M**≥3 events using the same criteria as Atkinson et al. (2016) (*i.e.* wells within 20 km and 90 days of the beginning of HF operations), working from an earthquake and well catalogue updated through the end of 2019. (Note: Comparing the 2009-2015 versus 2009-2019 time periods, the GA20 database is larger than that of Atkinson et al. 2016 by a factor of ~1.5). GA20 examined the distribution of the flagged **M**≥3 events in time and space with respect to the nearest candidate HF well. The empirical distributions were used to define a distance-based weight function (Wd) that has a maximum value of 1 for 0 distance,

decreasing to a value of 0.15 at 15 km. The distribution reflects the combination of the actual distance offsets between HF wells and events (<5 km) and location errors in the catalogue used (~5 km for most events, but up to 20 km for some events). A time-based weight function (Wt) has a value of 1 for a time lag of 0 days, decreasing to 0.15 for a lag of 60 days beyond the start of the time window for HF operations (where the time window for HF operations ranges from days to weeks, or occasionally months, such that in most cases the flagged events are occurring either within the HF window or within a few weeks following). The W score is taken as the average of the two values and is intended to provide a measure of relative likelihood of association. Based on a Monte Carlo analysis of the significance of the W score, GA20 concluded that, after accounting for the expected number of false positives, ~0.5% to 0.8% of HF wells in the WCSB (2009-2019) are associated with **M**≥3 seismicity, representing an association for approximately 50% of earthquakes. The 50% association percentage for earthquakes of **M**≥3 with HF wells is consistent with that found by Atkinson et al. (2016), but the average per-well association rate is higher than that found by Atkinson et al. (2016), by about a factor of two. The higher per-well rate may reflect inherent limitations of the W metric as originally implemented (*i.e.* an overcounting of wells associated with earthquakes) or could suggest that the percentage of wells that may be associated with observed seismicity has risen in the last few years. As described in the following, we explore both possibilities in this article.

A common thread in the three works (Atkinson et al., 2016; Ghofrani and Atkinson, 2016; 2020) is that we aim to characterize overall regional rates; we do not attempt to provide a definitive discriminant on an event-by-event or well-by-well basis. Such discriminations are better made using studies of smaller areas in which a rich sequence of earthquakes can be examined in detail with respect to surrounding operations – ideally with the help of microseismic and operational data provided by the operator or regulator (e.g. Wang et al., 2020; Rodriguez and Eaton, 2020; Schultz et al., 2017).

In this article, we build on the concepts of GA20 by incorporating improvements to the W metric and the databases it accesses. GA20 used the Composite Alberta Seismicity Catalogue (CASC; see Data and Resources) from 2009 to 2019. In this article, we use two catalogues that have recently become available: the Alberta Geological Survey catalogue (AGS), which is available from 2006 through 2020, and the northeastern B.C. catalogue (NEBC) of Visser et al. (2017; 2019), which is available from 2014 through 2019 (see Data and Resources). The new catalogues allow us to extend the study downwards in magnitude range to consider potential associations for events of **M**≥2. In addition to using a better database, we make several improvements to the W metric to address some of its inherent shortcomings, by tightening up the time and distance criteria to the extent feasible based on the available catalogues and HF well database information. We also address the potential influence of disposal wells, considering an analogous measure of this association. We compare the regional association rates for HF wells with expectations based on the seismicity database and previous studies. Finally, we use the improved metric to examine how the association between HF wells and seismicity varies with formation depth and age. This article therefore provides an update to the results of Ghofrani and Atkinson (2020) and includes additional information and data that informed a Comment and Reply to that article (Verdon and Bommer, 2021; Ghofrani and Atkinson, 2021).

Updated Seismicity Catalogues

The GA20 study used the Composite Alberta Seismicity Catalogue (CASC; Cui et al., 2016). We chose to consider only **M**≥3 events when using the CASC because it includes many undiagnosed blasts; there are very few blasts that register as **M**≥3 but blasts become a significant problem in some regions when using a lower magnitude threshold. In this study, we switch to two regional catalogues that are more uniform in their coverage and have fewer issues with blast contamination, enabling us to drop the magnitude threshold to **M**≥2, thus increasing the available seismicity database. We use the catalogue of the Alberta Geological Survey (AGS catalogue) and the Visser et al. (2017, 2019) catalogue for northeastern B.C. (NEBC catalogue) (see Data and Resources). Together, these catalogues cover most of the WCSB. We restrict the period of study from 2014 through 2019 as this is the time covered by the NEBC catalogue; the AGS catalogue is available from 2006 through 2020. We restrict the geographic area of study to those areas where the network coverage is best, which leads to more homogeneous location uncertainties. For example, the stated epicentral uncertainties in the AGS catalogue are as small as 1 to 2 km for recent events in well-sampled areas, but as large as 50 km for earlier events in northern Alberta (Gu et al., 2011; Stern et al., 2013). Location uncertainties in the selected study region are discussed in a following section.

AGS catalogue. We use **M**≥2 events from the AGS catalogue in the area from 51-57 N 113-120 W. The catalogue magnitude scale, ML (local magnitude), is converted to moment magnitude (**M**) as described in the next section. Figure 1 shows the study events (**M**≥2, 2014-2019) in the AGS catalogue. The number of stations used to locate the events has varied in time. In 2014, the mapped area was covered by ~ 9 stations, increasing to ~ 17 stations by 2018, with station density being greatest in the western half of the Foothills zone (FTH as defined for Canada's national seismic hazard maps by Kolaj et al., 2020; see Fig. 1). The AGS removes known blasts from its catalogue, which is a significant advantage over the CASC catalogue in this region if examining events of **M**<3.

NEBC catalogue. The best catalogue source for the northern portions of the WCSB is the NEBC catalogue compiled by Visser et al. (2017; 2019). Figure 2 shows the **M**≥2 study events for the region considered (55 – 58N; 120-124W). The northern cluster of the NEBC study area (north of 56.3) is only covered from 2014-2016, whilst the prolific southern cluster is covered from 2014 through 2019. The solutions come from ~30 regional stations, including 6 stations that lie within the study area shown on Fig. 2. Magnitudes were converted from ML to **M** (next section). The NEBC catalogue includes blasts and events that are related to mining, as discussed by Dohkt et al. (2020). However, such events do not affect those flagged as potentially associated with HF wells in the study area, because the flagged events are not in proximity to known mining operations and show no correlation with known blasting times.

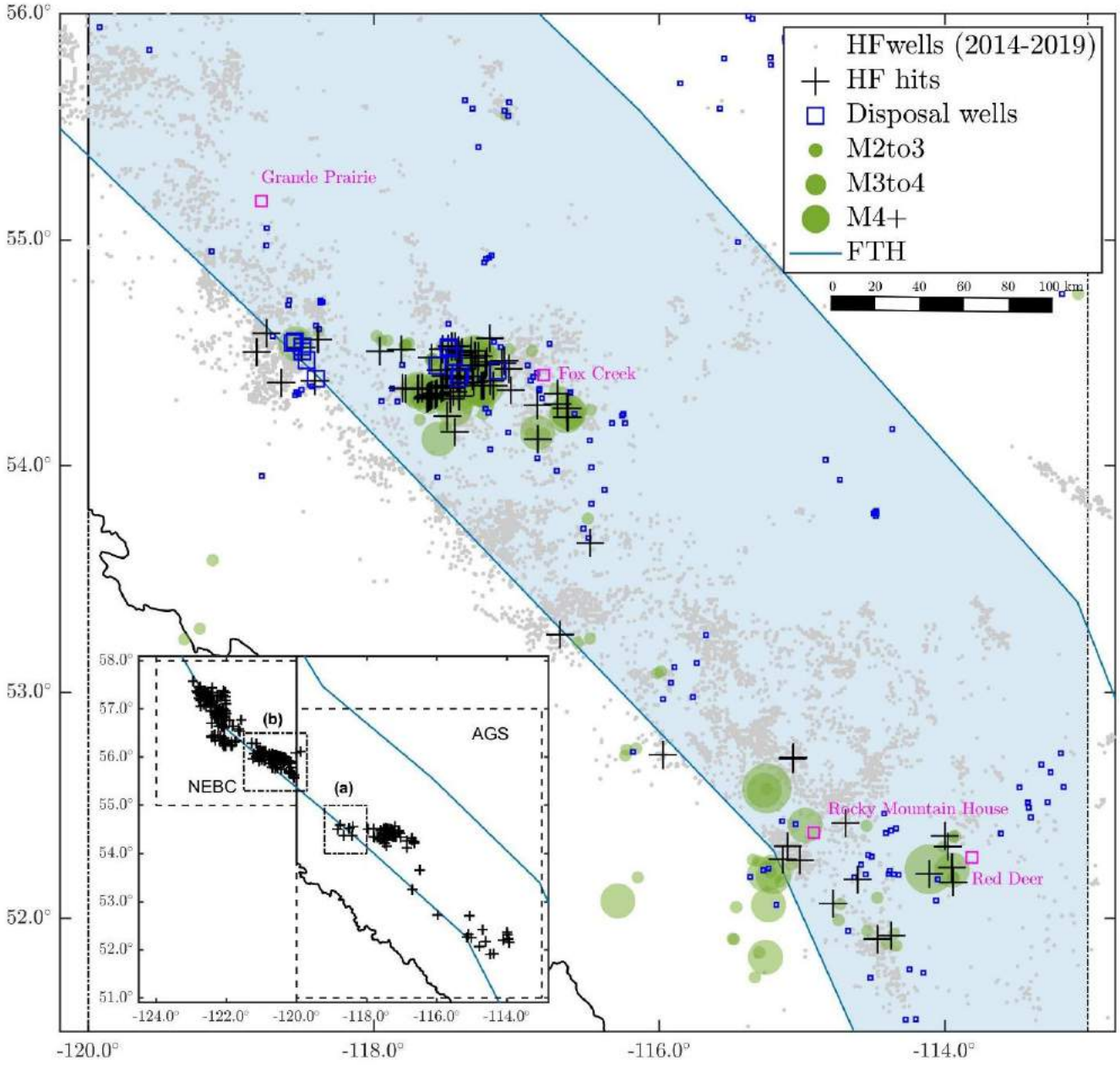

*Figure 1 – Events of **M**≥2 in the AGS catalogue (in area from 51 to 56N) from 2014 through 2019 (circles). Background is all HF wells 2014-2019; plus symbols show HF well hits (next section). Disposal wells (2014-2019) shown by squares, with larger squares showing those that may be associated with seismicity (Ww>=0.20). The Foothills (FTH) areal source zone (Kolaj et al., 2020) is shaded. Inset shows entire study area (NEBC and AGS, with FTH zone shown by lines; hits are shown by + symbol). Small boxes within insets highlight areas discussed later.*

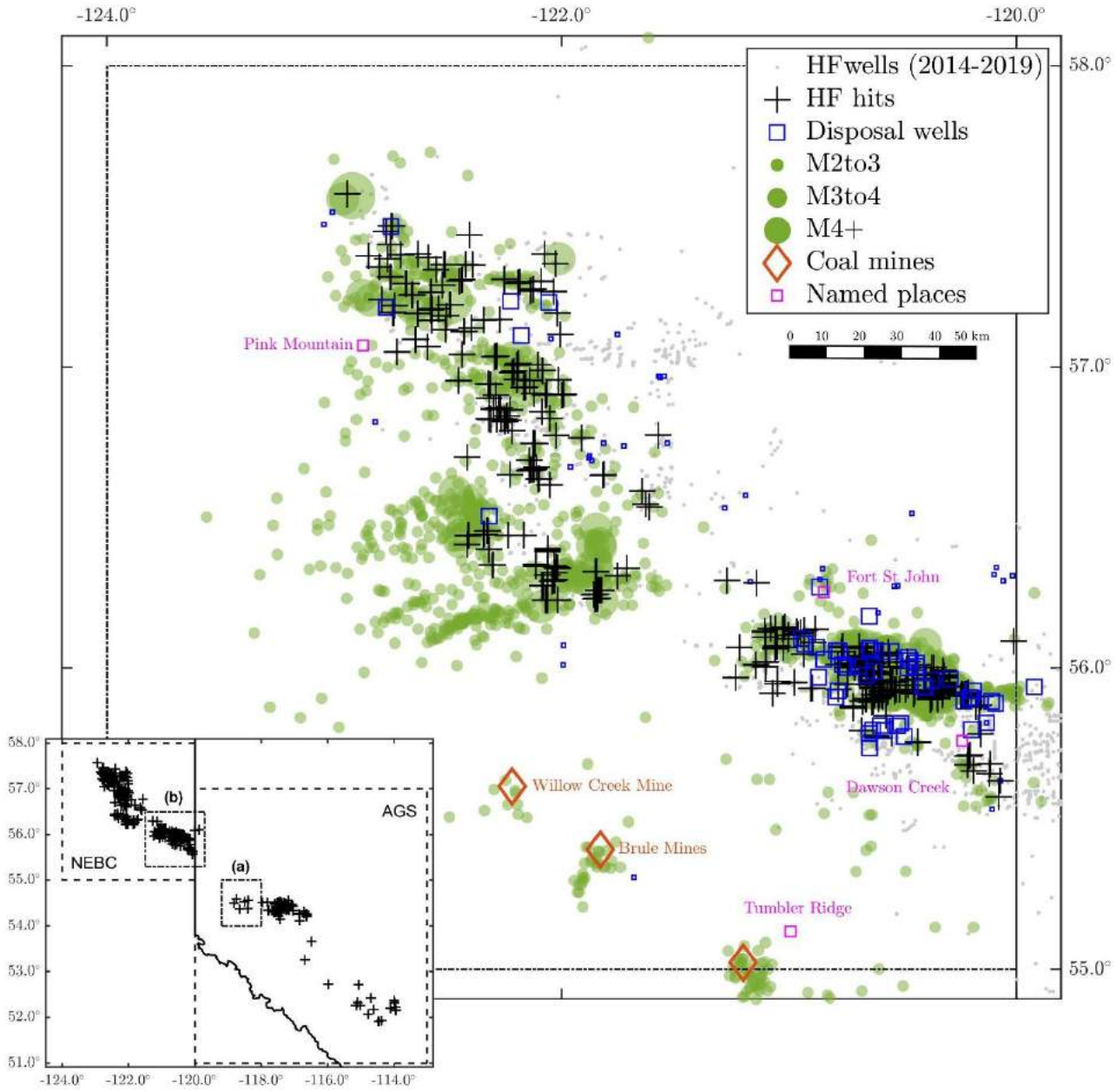

*Figure 2 – Events of **M**≥2 in the NEBC catalogue (in area from 55 to 58N) from 2014 through 2019 (circles). Background is all HF wells 2014-2019; plus symbols show HF well hits (next section). Diamonds show mines associated with seismicity. Disposal wells (2014-2019) shown by squares, with larger squares showing those that may be associated with seismicity (Ww>=0.20). Inset shows entire study area (NEBC and AGS; events that are hits are shown by + symbol). Small boxes within insets highlight areas discussed later.*

Moment Magnitude Conversions. The AGS and NEBC catalogues both report ML magnitude, but their calculation methods are not identical so the two measures of ML may not be equivalent. Moreover, the AGS changed from use of the Hutton and Boore (1987) attenuation correction to

the Yenier (2017) formula in 2018, resulting in a change in the meaning of ML in the AGS in 2018. To place all events on a common scale, we convert all magnitudes to moment magnitude (**M**). Many of the study events have values of **M** values that were determined by inversion of regional spectral data by Holmgren et al. (2020), who showed that their **M** values agree well with those of regional moment tensor solutions on average. However, for the largest events (**M**>3.5) we noted that there is a tendency for the Holmgren et al. (2020) values to be lower than the corresponding values from regional moment tensors, such as those reported by the Pacific Geoscience Centre (PGC). On the other hand, the PGC values may be an overestimate; they often report **M**>ML, whereas we would expect that **M**=ML on average for events of **M**~3.5 to 4. To stabilize estimates of moment for the larger events, we take the average of all available **M** values, which include those of Holmgren et al. (2020); PGC; Wang et al. (2018) and Zhang et al. (2016); there are up to 3 values for the larger events (**M**>3.5), whereas for small events (**M**<3) the **M** estimates are entirely from Holmgren et al. (2020).

We developed empirical correlations between ML and **M** for each catalogue, based on 52 events in the AGS catalogue having determined **M** values, and 45 events in the NEBC catalogue. Figure 3 shows the developed correlations, which can be summarized as follows:

1. For the AGS catalogue, ML=**M** for 2018 onwards.
2. For the AGS pre-2018, **M** = ML - 0.29 (derived using pre-2018 events with 2.5≤ML≤4.8).
3. For the NEBC catalogue, **M** = ML+ 0.3 (derived using entire **M** range).

The standard deviation of the estimate of **M** from ML for the AGS and NEBC catalogues is 0.28 and 0.29, respectively. These relationships are used to place all events in this study on a common magnitude scale (**M**). However, this step is not critical as magnitude is used only as a screening threshold for our study (*i.e.* we examine events with **M**≥2).

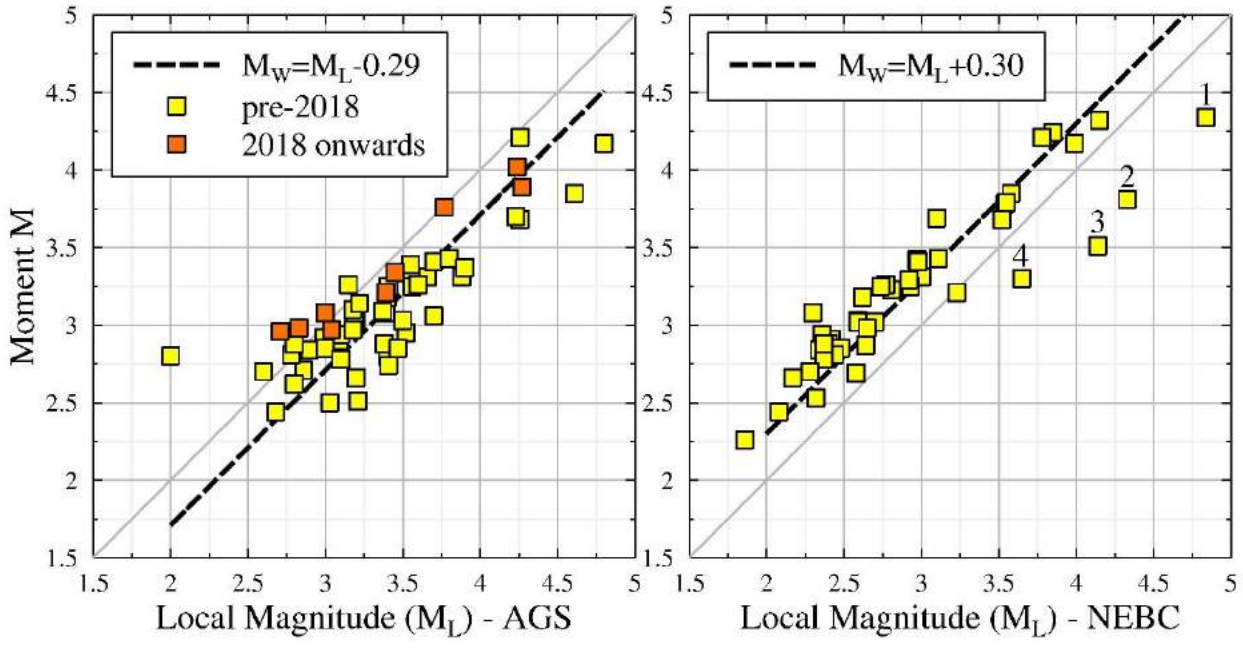

*Figure 3 – Empirical correlations between **M** and ML for AGS and NEBC catalogues. Note that there are 4 (numbered) NEBC events with large ML relative to assigned **M**; these are the 2018/11/30 events (Mahani et al., 2019) and the 2015/11/03 event.*

Location Uncertainties. Uncertainty in hypocentral location is a major factor in assessing the potential for association between HF wells and earthquakes. Most HF-associated events are expected to be within a few km of the well (e.g. Schultz et al., 2017; Rodriguez and Eaton, 2020; Wang et al., 2020). However, HF wells may be significantly further away from the earthquake locations given in the catalogue. In areas where the station coverage is good, the epicentral location errors may be only a few km and so we would expect most events to be located within ~5 km of wells. But the location error varies significantly across the region, resulting in many cases where potentially associated events appear to be at greater distances from HF wells. Moreover, since events can trigger other events, there is a potential for the area of associated events to expand beyond the initial range of influence of the well. Due to the sparse network density, hypocentral depth is poorly determined for most events. In this section, we assess the location uncertainties for the events in our study catalogues.

An initial estimate of location errors can be obtained by examining the statistics of the error ellipses provided by regional catalogues. The NEBC catalogue reports small error ellipses, with the major axis error having a mean of ~1.5 km and standard deviation of ~1.5 km. However, Visser et al. discarded all events having a semi-major axis error of >10 km in compiling the catalogue, and thus these uncertainties may be an underestimate of the network's general location accuracy. Dokht et al. (2020) performed a detailed inversion analysis to better characterize location uncertainty within the NEBC catalogue (using the NonLinLoc algorithm of Lomax et al., 2000); their analysis suggests location uncertainty of ~11 km, much larger than that suggested by the error ellipses.

The AGS catalogue does not report its error ellipses. However, its location uncertainty should be comparable to that of the Nanometrics catalogue for the central Alberta region (see Data and Resources). The Nanometrics catalogue in central Alberta uses the AGS stations plus several additional private stations that improve coverage in the areas near several major dams. While the locations of many events since 2014, as reported in the Nanometrics catalogue, are constrained to within a few km, it is not uncommon for the length of the semi-major error axis to exceed 10 km. The error ellipses in central Alberta are quite asymmetric due to azimuthal gaps in station coverage. For events of **M**>2.5 in the Nanometrics catalogue, the semi-minor error ellipse has a mean of 1.8 km and standard deviation of 1.8 km. However, the semi-major error ellipse has a mean of 9 km, with standard deviation of 9 km. The median length of the major axis is 5 km, with the 75^{th} and 95^{th} percentiles being 16 km and 28 km, respectively. Thus, if we consider the size of error ellipses and the potential triggering distances, an initial expectation is that most events would be located within 10 km of the corresponding HF well, but that larger errors are not uncommon.

A shortcoming of using the error ellipse to characterize location uncertainty is that it measures only the within-model error and thus does not consider the effects of uncertainty or heterogeneity in the velocity model or the effects of random errors such as those in phase picking. One way of assessing the effects of these uncertainties is to compare locations from alternative networks that are comparable in network coverage and quality. Such a comparison can be made using the AGS and Nanometrics catalogues. For central Alberta, the distance between event locations within these catalogues is on average 5 km with a standard deviation of 4 km. Thus, it is not unusual for the epicenters in the two catalogues to be 10 km or more apart. Ghofrani and Atkinson (2021) provide an illustrative example for an example cluster of events in central Alberta.

Another catalogue-to-catalogue comparison can be made in the region of Fox Creek, Alberta, which is covered by both the AGS and NEBC catalogues. We adopted the AGS catalogue in this region, but a comparison with the NEBC locations is useful. A comparison of event locations shows that the overall activity patterns agree between the two catalogues, but that some events are >15 km apart, despite the small (<2 km) error quoted by the NEBC catalogue.

Our conclusion is that in most cases we would expect to see events located within ~5 to 10 km of associated wells, at least within the last few years. However, some events may appear to be as far as 20 km away due to event mislocations. This uncertainty can be represented by the distance weighting score in the W metric. As shown in the next section (Figure 4), a high value of W is given to events within 5 km, but association may still be possible to larger distances, with decreasing likelihood, due to the issues noted above.

Refinements to the W metric and its interpretation

The use of improved regional seismicity catalogues allows us to re-examine the W metric as defined in GA20 for HF wells and refine it as warranted. We also explore an analogous metric for disposal wells. Finally, we address a shortcoming in the original W metric by calibrating it in an overall sense to adjust for any overcounting of events per well.

Refined W Metric for HF wells

Starting from the new seismicity catalogues of the AGS and NEBC (Figures 1 and 2), we flag all events of **M**≥2 within 20 km and 90 days of the initiation of HF activities at a well. For each flagged event, we calculate the weight for distance for each flagged HF well, using the same function defined in GA20, which has a value of 1.0 at 0 distance, decaying to 0.10 at 20 km:

$$W_d = \begin{cases} 1.0 & D \leq 3\ km \\ 3.794D^{-1.2137} & D > 3\ km \end{cases} \quad (1)$$

We considered refining the Wd function to provide a stricter measure of association due to distance. For example, we considered limiting the distance of potentially associated events to 10 km. However, we decided against this restriction for two reasons. The first is that, based on our investigation of event location uncertainties, we concluded that some associated events may appear to be at greater distances. The second reason is that, in our preliminary investigations, we discovered that imposing a tighter (e.g. 10km) offset criteria results in many earthquakes that are not flagged, but appear very close in both space and time to flagged events, in a clustered fashion. This may be due to inaccuracies in location or to migration of activity in space over time. An intriguing possibility is that triggering may be acting over larger distance scales (i.e. remote triggering may be more widespread than recognized) (e.g. van der Elst et al., 2013; Wang et al., 2015, 2019; Dohkt et al., 2020). In view of these observations, we have not tightened the distance criteria, instead considering the probability of association for events at 20 km to be low but non-zero.

In this study, we refine the measure of the time lag. A simplification made in GA20 was to measure lag time relative to the start date of the HF window, without reference to the individual stages within the HF window or to the end date of the HF operations. This conceptual shortcoming caused a lack of transparency in our original paper regarding the timing of events

relative to operations (as pointed out by R. Skoumal, pers. comm., 2019). Though most of our flagged events occurred within the HF window, many were listed as having significant lags because the length of the HF window can range from a few days to a few months. To reduce this ambiguity in timing, we refine our metric here by measuring the time lag relative to the most recent previous stage of fracking; this makes the timing of events relative to operations more transparent and shows that most hits are within days, and almost all within a few weeks, of the associated HF operations.

Figure 4 compares the distribution of lag times for our original function of GA20 (Wt1), which was measured relative to the start of HF operations, to our new function (Wt2), which is measured relative to the most recent frack stage. Because of the change in how lag time is defined, we obtain a much tighter distribution, with a more rapid decay in time. We represent this as:

$$W_{t2} = \begin{cases} 1.0 & D \leq 1\ day \\ T^{-0.76862} & D > 1\ day \end{cases} \quad (2)$$

As seen on Figure 4, a value of Wt1=0.35 (GA20 study) represents a lag time of ~19 days with respect to the initiation of HF operations but is equivalent to a lag of only ~4 days with respect to the most recent frack stage (as measured by Wt2=0.35). Figure 4 makes clear that, for Wt2=0.35, most hits are within a few days and almost all are within 1 month of HF operations. For example, Wt2=0.15 is reached 20 days after the most recent frack stage; by comparison, the value of Wt1=0.15 was reached 60 days after initiation of HF operations.

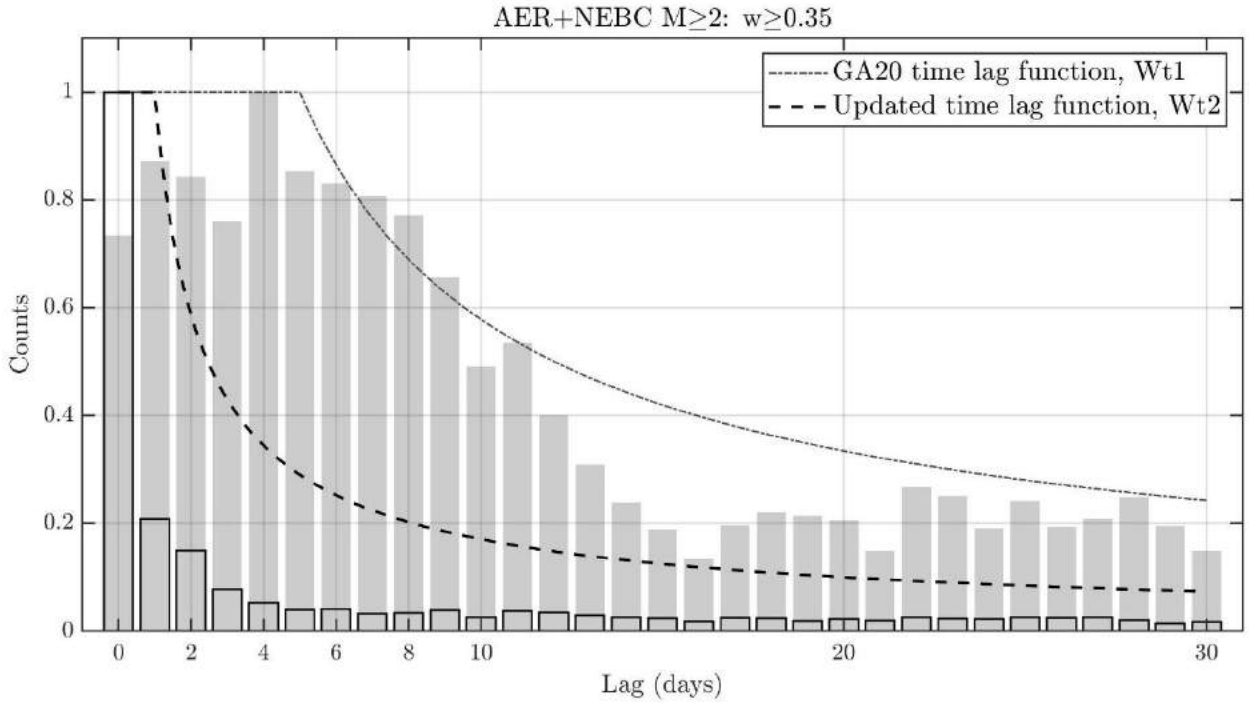

Figure 4 – Comparison of lag times for flagged events based on the GA20 function (Wt1), which is measured relative to the initiation of HF operations (grey shaded bars), to lag times based on the new function (Wt2; Eqn. 2) (black outlined bars). The distributions are shown based on all HF wells with Wt1 (or Wt2) >0.35.

We calculate Wd and Wt2 for each HF well that passes the initial screening criteria for all events of **M**≥2 and calculate W as the average of the two scores. Figure 5 summarizes the distribution of hits for the highest scoring HF well near each event in both time and space in comparison to the adopted Wd and Wt2 weighting functions. Figure 6 shows the corresponding distributions for all HF wells for which W≥0.35. The counts are normalized to reach a maximum value of 1.0, by dividing by the maximum bin count for each panel (Nmax=741 for offsets and 3491 for lag time on Fig. 5; Nmax=3870 for offsets and 23,880 for lag time on Fig. 6). The highest scoring HF wells are within 10 km and 10 days of the HF operations, as we would expect based on the way the weighting functions are defined. If we consider all wells with W≥0.35, to reflect uncertainty in the true locations of events and potential ambiguity in their attribution, we obtain broader tails, especially in the distance distribution. Some of the HF wells in these tails will represent false positives, as the events may be related to a higher scoring well or be coincidental. However, given the significant mislocations for some events, the highest scoring well may not always be the culprit well. Moreover, there may be some events for which multiple factors are involved in triggering – such as the combination of a disposal well and a nearby HF well. We explore these issues in a later section.

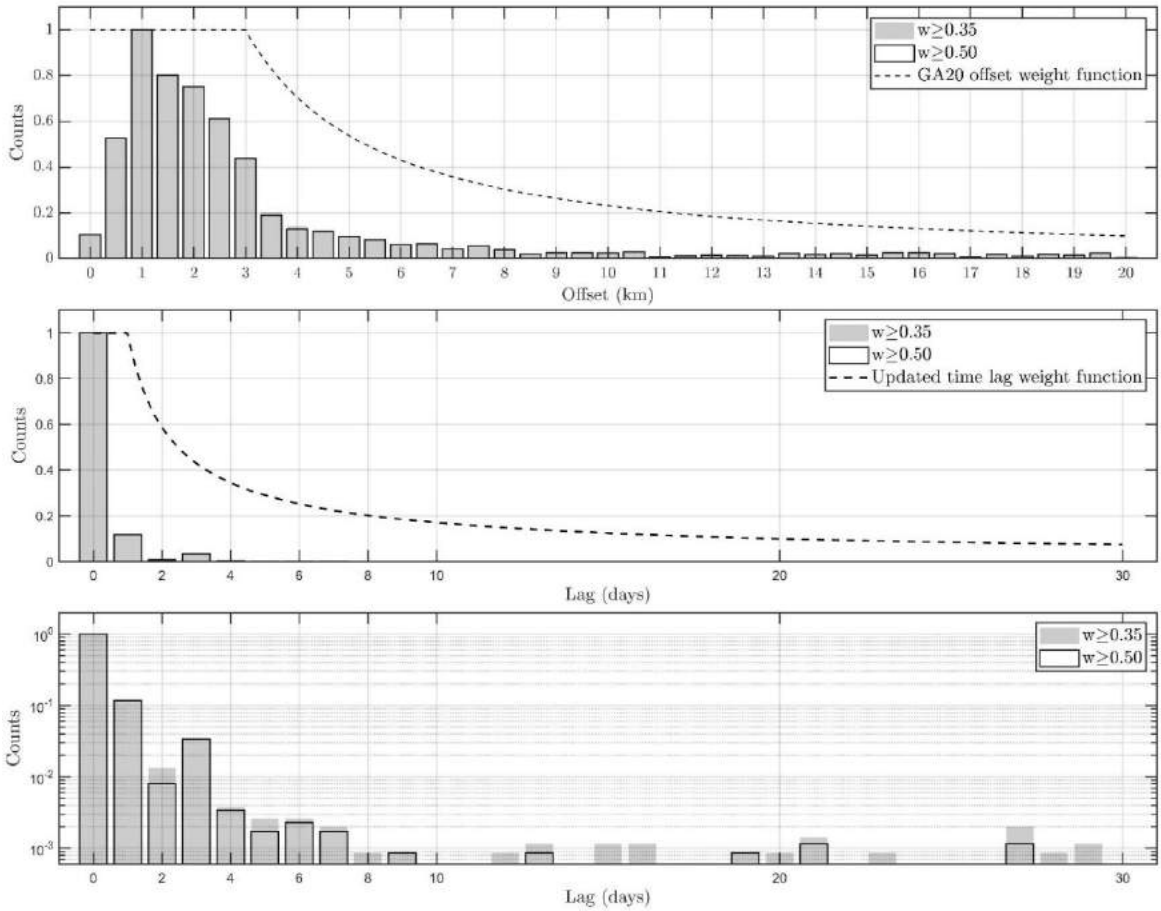

*Figure 5 - Distribution of W scores in time and distance for the AGS and NEBC catalogues combined, for events with W≥0.35; for events having multiple hits, the plot uses the highest-scoring HF well. Black bars show counts for W≥0.50. Top: Distribution of closest distance from event to highest-scoring HF well. Middle: time lags of **M** ≥ 2 events associated with highest-*

scoring HF wells. Bottom: same as middle panel but shown on log scale. Lines show W metric adopted in this study (Wd as in GA20, with maximum value=1.0, minimum=0.15; Wt2 as per Eqn 2, with maximum=1.0, minimum 0.10).

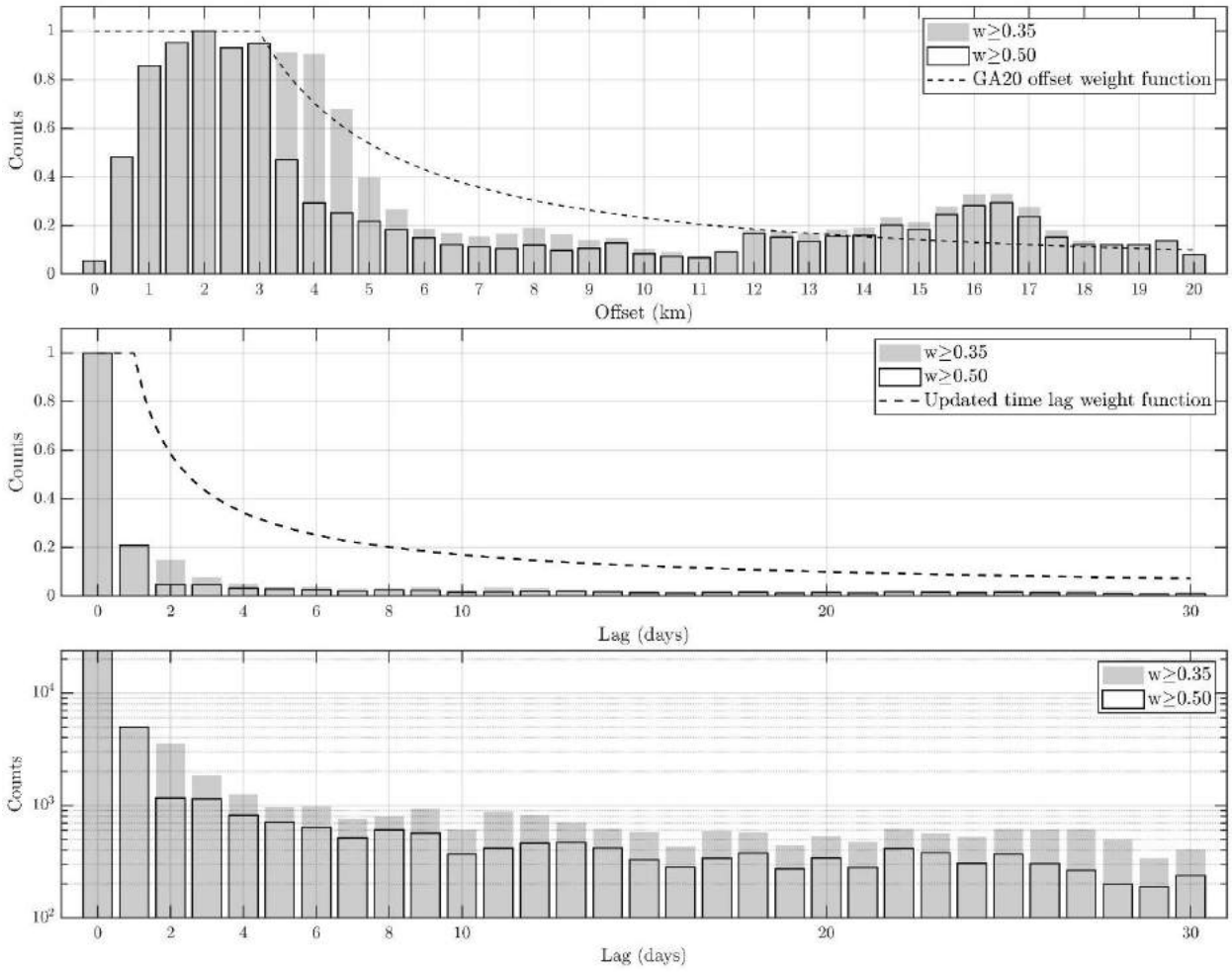

*Figure 6 - Distribution of W scores in time and distance for the AGS and NEBC catalogues combined, for all events with W≥0.35 (not just those with the highest score). Black bars show counts for W≥0.50. Top: Distribution of closest distance from event to HF well. Middle: time lags of **M** ≥ 2 events associated with HF wells. Bottom: same as middle panel but shown on log scale. Lines show W metric adopted in this study (Wd as in GA20, with maximum value=1.0, minimum=0.15; Wt2 as per Eqn 2, with maximum=1.0, minimum 0.10).*

Overall, the W metric has not changed dramatically from that defined in GA20 but has been refined. We consider W=0.35 as a reasonable threshold for potential association of seismicity with HF wells. On average, such wells are located within 8 km and 4 days of the corresponding events. However, for an event on the same day as the HF operations, the catalogue location could sometimes be as far as 20 km from the well. On the other hand, for an event located <3 km from an HF well, the time lag could be as much as 30 days after the HF operations. These time and distance scales are consistent with the range of associations between events and HF wells reported in the literature, in view of the location uncertainties as discussed in the foregoing. We recognize that some of the events will represent false positives. On the other hand, there are

many events with W<1 that are effectively undercounted for association (i.e. true associations that are only partially counted). The balancing of these opposing trends is discussed in a later section. The Appendix table lists all **M**≥2 events that are potentially associated (at 0.35 threshold) with HF wells (and/or disposal wells) and provides metrics for the wells with highest association score.

Development of W Metric for Water Disposal Wells

The GA20 studied focused exclusively on the potential association between HF wells and earthquakes. However, it is known that in some areas most of the seismicity is associated with water disposal wells (e.g. Schultz et al., 2014). There may also be areas where an association appears plausible for both HF and disposal wells (e.g. Atkinson et al., 2016). We explore applying the W metric to express the likelihood that events are related to nearby disposal wells. A challenge is that the time scales of the disposal and HF processes are markedly different, as disposal wells often operate for many years whereas HF operations are short-term. The distance scales may also potentially differ due to the large cumulative volumes of water that may be disposed over time, resulting in an expanding pore pressure signature around a disposal well.

To define a W metric for disposal wells, we begin by examining the distribution of **M**≥2 events within 20 km of disposal wells during their operational period (i.e. starting with first date of operation and ending with date of well closure + 90 days). Due to the long duration of operations (i.e. over years), an association between a disposal well and seismicity is only considered likely if there have been multiple potentially associated events over the operational period. We express this by defining a metric that expresses an event rate, weighted by distance. We search for events near disposal wells, rather than searching for wells near events (as we did for HF wells). For each **M**≥2 event within 20 km of a disposal well, we calculate Wd (Eqn 1) and sum these values over all events for that well (=Wdsum). We then divide Wdsum by the number of operational months (within the timeframe of the corresponding earthquake catalogue being examined, where a month is 30 days), to make the time scale roughly equivalent to that used for HF wells (i.e. events associated with HF wells occur within a 1 month time frame). The maximum value of (Wdsum/#months) that we obtained over all wells was much higher for the NEBC catalogue (45.7) than for the AGS catalogue (0.837). This reflects the higher event productivity in the NEBC catalogue compared to the AGS catalogue; for example, the maximum number of **M**≥2 events within 20 km of a disposal well is 1526 for the NEBC catalogue compared to 30 for the AGS catalogue.

The maximum value of Ww (a measure of the likelihood that the well is associated with seismicity) should not exceed 1 on a per well basis. Thus we take Ww to be the minimum value of Wdsum/#months or 1.0. The distribution of Ww scores obtained for the disposal wells are shown as a function of distance from the *nearest* associated event in Figure 7; note that many other events that contribute to the Ww score for the well will be located further away (up to 20 km). Based on evaluation of this distance distribution, we consider a minimum reasonable threshold to consider a potential association of Ww=0.20; most such disposal wells have at least 1 event within 10 km. There are 14 wells for the AGS catalogue and 58 wells for the NEBC catalogue flagged using this criterion, as indicated on Figures 1 and 2. The Ww metric is not by itself diagnostic of an association, given the lack of restriction on timing and the high likelihood of a significant Ww value whenever a disposal well lies with an area of prolific seismicity (by manner of its definition). Its main utility is in flagging such disposal wells so that nearby events

that were flagged for HF can be examined further. Events potentially associated with HF wells that may have a stronger association with a disposal well (Ww>W) are indicated in the appendix table (Table A1), with the Wd value for the event relative to the disposal well being provided. Note that we have flagged disposal events in Table A1 only if they have Wd≥0.35, for consistency with the HF flagging; however, all events within 20 km of the disposal well were used in calculating Ww.

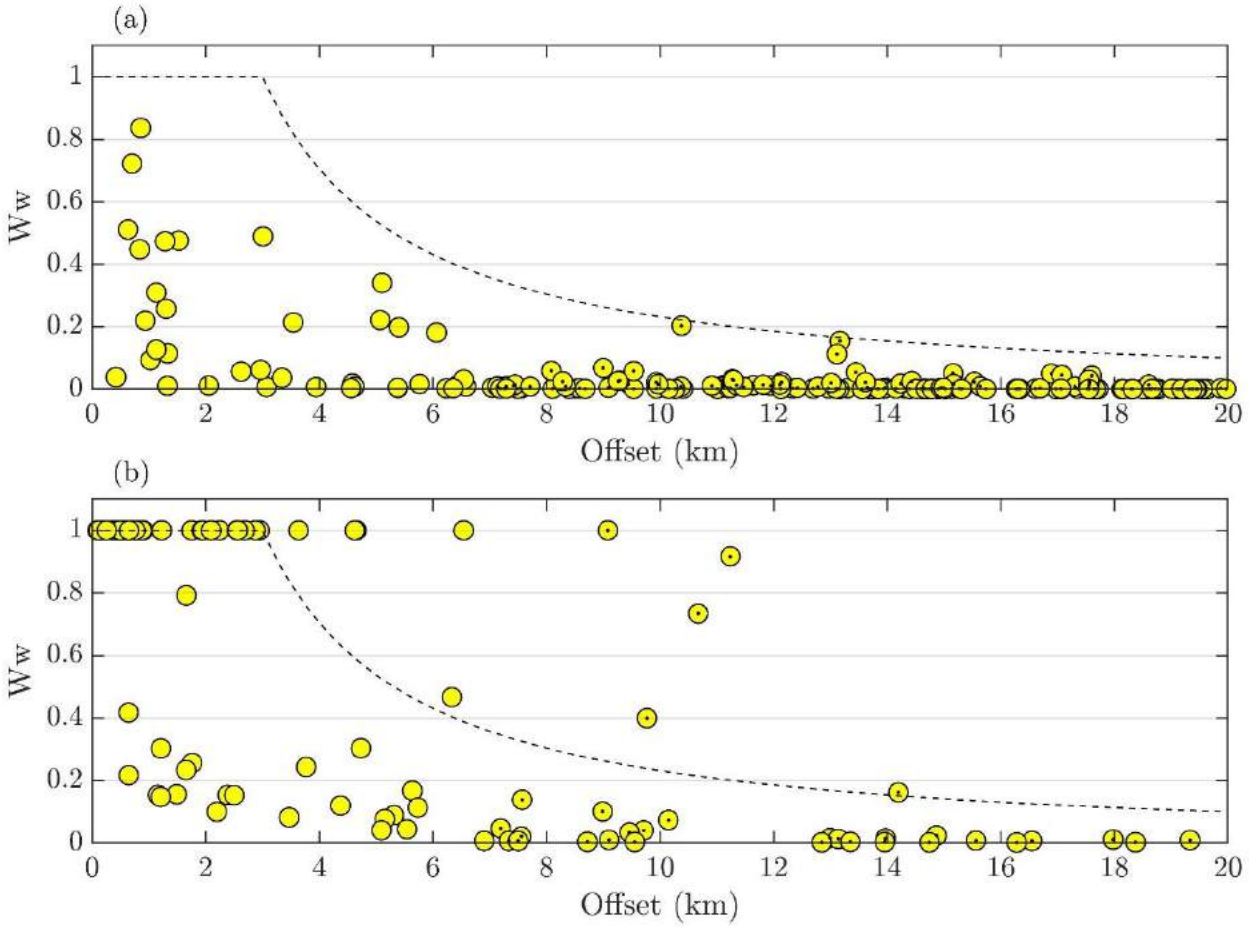

*Figure 7 – Distribution of Ww scores, based on the event at closest distance, for the (a) AGS and (b) NEBC catalogues, for all disposal wells having events of **M**≥2 within 20 km during its operational period. The black dashed line is the GA20 Wd model. The offset is the distance to nearest well. Symbols with dots show wells for which the nearest event did not pass the Wd≥0.35 threshold.*

Updated Association Potential and its Interpretation

We consider two methods of using the W scores to calculate the regional association rates between wells passing the minimum threshold for association significance and earthquakes of **M**≥2. One way is to consider just the highest scoring well associated with each earthquake, and

count only its highest-scoring earthquake, thereby avoiding any double counting of either wells or earthquakes. A drawback of that approach is that many events are ambiguous, with similar scores for several HF wells and/or several disposal wells, and thus the association of the event with the highest scoring well is partly arbitrary. An alternative approach that addresses this problem is to count the W scores for all events over all wells. This counts each event only once, but has the potential to overcount wells, as some events are potentially associated with several wells. This drawback can be addressed by correcting the well counts by an overcount factor (i.e. such that the average W value per well does not exceed 1). Note that both these approaches are more straightforward than that taken by GA20; GA20 counted the number of hits above a given W threshold, then used a Monte Carlo simulation to estimate the false positive rate for that threshold and adjust for it accordingly. The common element in all approaches is the use of an objective measure of spatiotemporal association, adjusted for an expected rate of false positives. In this study, we will demonstrate that this approach provides results that are entirely consistent with the observed seismicity patterns in the region.

Under the first approach, we organize the earthquake hits having $W \geq 0.35$ by the corresponding HF wells (Table 1 A). For each such event, we consider only the highest-scoring HF well of those that are potentially associated. For each such well, we take its highest-scoring earthquake (if there is more than 1). Summing these scores over all HF wells (with no double-counting of wells or earthquakes), we obtain *Wsum*=86.6 for the AGS catalogue and *Wsum*=410 for the NEBC catalogue.

The total number of HF wells considered for the two catalogues is 9300 (AGS) and 2500 (NEBC) (2014-2019 southern area; 2014-2016 northern area). Based on our *W* sums as organized by HF wells, this gives an apparent regional rate of association rate (*i.e.* a per well activation rate) of 0.9% for HF wells in central Alberta (i.e. =100*86.6/9300), and 16% for HF wells in NEBC, for events of $\mathbf{M} \geq 2$. These rates are based on no double counting of either earthquakes or wells, and only partial counting of the associations for most events ($W<1$). These percentages may initially appear high compared to previous studies (e.g. Atkinson et al., 2016 found a rate of 0.3% for $\mathbf{M} \geq 3$), especially for NEBC, but note that: (i) the magnitude threshold is lower than that used in previous studies; and (ii) seismicity has been very prolific in NEBC in recent years.

Many HF wells are potentially associated with more than one earthquake. If we sum the highest event scores over all potentially associated wells (i.e. such that each well is associated with only one earthquake, but each earthquake may be associated with multiple wells), we obtain *Wsum*=181 for AGS and *Wsum*=916 for NEBC. By comparison with our best-earthquake, best-well tally, we infer that this may result in an overcounting of wells per earthquake by as much as a factor of 2.09 (=181/86.6) for AGS and 2.23 (=916/410) for NEBC.

Another way to aggregate the *W* scores is to sum the highest well scores over all potentially associated events (i.e. such that each earthquake is associated with only one well, but each well may be associated with multiple earthquakes). In this case we obtain *Wsum*=280 for the AGS catalogue and *Wsum*=3888 for the NEBC catalogue. This implies that there is an average of 3.23 $\mathbf{M} \geq 2$ events per associated HF well for central Alberta (=280/86.6) versus 9.48 events per HF well for NEBC (=3888/410). The potentially associated HF events account for 56% of all $\mathbf{M} \geq 2$ events in the AGS catalogue for the study period (280 of 503 events) and 70% of events in the NEBC catalogue (3888 of 5560 events).

Finally, by taking the product of the activation rate and the event rate per well, we obtain a per-well rate of events of **M**≥2 of 0.030 for the AGS catalogue (=0.009*3.2 events per hit well), or 1.52 for the NEBC catalogue (=0.16*9.5 events per hit well), with no double counting of either earthquakes or HF wells. We can scale these rates for larger magnitudes, by assuming a Gutenberg-Richter distribution with a slope of 1 (Eaton et al., 2018; Shcherbakov et al., 2020). For example, the corresponding per-well event rates for **M**≥3 would be 0.003 for central Alberta and 0.15 for NEBC.

An alternative method of counting association rates for HF wells is to organize the hits having $W \geq 0.35$ by events (Table 1 B). For each **M**≥2 event, we sum *W* over all qualifying HF wells ($W \geq 0.35$). If $Wsum \leq 1.0$, there is no apparent overcount of association for that event and we adopt *Wsum* as representative of its association potential (*i.e. Wev=Wsum*). If $Wsum > 1$, we know we are overcounting associated HF wells for that event and instead set $Wev = 1$. The overcount factor, if we count over all events and all potentially associated HF wells, is $\sum Wsum / \sum Wev$, where the summation ($\sum$) is taken over all potentially associated events.

Following this logic, for the events having $W \geq 0.35$ in the AGS catalogue we obtain an overcount factor of 3.8 (=917/239), if all well scores (not just the highest) are counted for each event. For the more prolific NEBC catalogue, the overcount factor is 8.5 (=32,479/3557).

We can divide $\sum Wev$ by the total number of HF wells (9300 for AGS, 2500 for NEBC) to calculate the per well hit rate, which is 0.026 for the AGS catalogue and 1.53 for the NEBC catalogue. Note that these rates are associated with events of **M**≥2. For a Gutenberg-Richter relation with a slope of 1, event rates per well would be 10 times lower for **M**≥3, 100 times lower for **M**≥4, and so on. Based on the event and association counts, we infer that ~48% of **M**≥2 events in the AGS catalogue (503 events), and ~69% of events in the NEBC catalogue (5560 events), are associated with HF wells. These rates are generally consistent with the corresponding rates obtained by counting just the highest scoring wells (56% for AGS, 70% for NEBC), providing confidence that the estimated percentages are robust, and that we can correct for any overcounting that occurs.

In Table 1, we present the summary of potential association statistics based on the foregoing descriptions (where the indices are used to show how the values are calculated). We conclude that the average regional likelihood of association of HF wells with **M**≥2 seismicity, from 2014-2019, is ~0.9% per well in central Alberta, and ~16% per well in NEBC, with no double-counting of either earthquakes or wells. Overall, HF wells are associated with ~50% of all observed **M**≥2 seismicity in Alberta, and ~70% in NEBC.

*Table 1 – Summary of Regional Statistics for Potential Association of HF wells with **M**≥2 earthquakes in the Western Canada Sedimentary Basin (2014-2019)*

A. Organized by HF Wells	index	AGS	NEBC
#wells (total)	i1	9300	2500
Sum W (best well, best event)	i2	86.6	410

Hit rate (per well) (=i2/i1)	i3	0.009	0.164
Sum W (best well, all events)	i4	280	3888
Sum W (all wells, best event)	i5	181	916
Overcount (=i5/i2)	i6	2.09	2.23
N(M>2) per hit well (=i4/i2)	i7	3.23	9.48
N(M>2) per well (=i3*i7)		**0.030**	**1.554**
N(M>2) catalogue	i8	503	5560
Fraction N(M>2) (=i4/i8)	i9	**0.56**	**0.70**
B. Organized by Events			
#hits W>0.35 (total)	i10	251	3888
Sum W (best well)	i11	212	3557
Sum W (all wells, all events)	i12	917	32479
Sum W (max=1)	i13	239	3835
Overcount (=i13/i12)	i14	3.84	8.47
N(M>2) per well (=i13/i1)	i15	**0.026**	**1.534**
Fraction N(M>2) (=i15*i1/i8)	i16	**0.48**	**0.69**

The regional rate of association of HF wells with **M**≥3 seismicity for the WCSB reported by GA20 (0.8%) can be compared to the results of Table 1 with some further manipulation. To do this we filter the hits in our updated study to include only **M**≥3 events. If we sum the *W* scores over all wells that register as hits (with *W*>0.35), counting each well no more than once (and imposing a maximum of *W*=1 for each event), we infer a regional hit rate for **M**≥3 of 0.2% for Alberta (22 of 9300 wells) and 4% for NEBC (98 of 2500 wells). If we combine Alberta and NEBC, this implies an average regional per well activation rate for **M**≥3 events of ~1% (120 of 11800 wells), which is consistent with the result of GA20. As was demonstrated in the main text, these rates are also consistent with expectations based on observed seismicity rates versus time, broken down by their contribution components (HF, disposal, natural).

Finally, we conduct a sensitivity test to determine how the results of Table 1 would change if we assumed a cut-off distance of 15 km for potential association (instead of 20 km). Referencing the well counts of Table 1, *Wsum* for the best well, best event (i2) would reduce to 79.4 and 384 for the AGS and NEBC catalogues, respectively. This would reduce our per-well hit rates (i3) by only 8% and 6%, respectively (e.g. from 0.009 to 0.008 for AGS; from 0.164 to 0.154 for NEBC). If we consider *Wsum* for all wells, best event (i5), we obtain a reduction of 15% in the overall count for the AGS catalogue; however, this is partially compensated by a reduction of 8% in the overcount factor, such that the inferred hit rate is reduced by only 7%. For the NEBC catalogue, considering all wells, best event, the 15 km cut-off would likewise result in a

reduction in the hit rate of only 7%. We conclude that the regional hit rates we obtain are not overly sensitive to the 20 km cut-off for association.

Contributions from Wastewater Disposal Wells: The interpretation of the wastewater disposal well scores is challenging, as *Ww* simply flags wells with significant **M**≥2 seismicity within 20 km. *Ww*=1 corresponds to 1 or more events/month, while the minimum significant value of *Ww*=0.2 represents ~2 events/year. We use *Ww* only to revisit the significance of the earthquakes flagged for potential association with HF wells. A simple confirmation of the significance of the *W* value for a HF-associated event is that it exceeds *Ww*. For Alberta, this check suggests that only ~2% of HF flagged events are also credible candidates for disposal wells; in NEBC, ~25% of HF flagged events may also have a credible link with disposal. The discrepancy by region reflects the greater density of earthquakes in NEBC, including an area of high seismicity that contains both disposal and HF wells. By examining the events that are potentially associated with both HF and disposal wells, we observe that the great majority of these fall into a small area within each catalogue, as illustrated in Figures 8 and 9. In these areas, we speculate that in some cases there may be an interaction, in which a disposal well decreases effective stress, and then an HF well triggers events. We do not attempt to diagnose the details of the associations in these areas, as that goal would be better achieved through detailed studies of specific sequences, using more detailed information. Outside of the areas shown in Figures 8 and 9, the HF hits do not appear to have a credible link to nearby disposal wells.

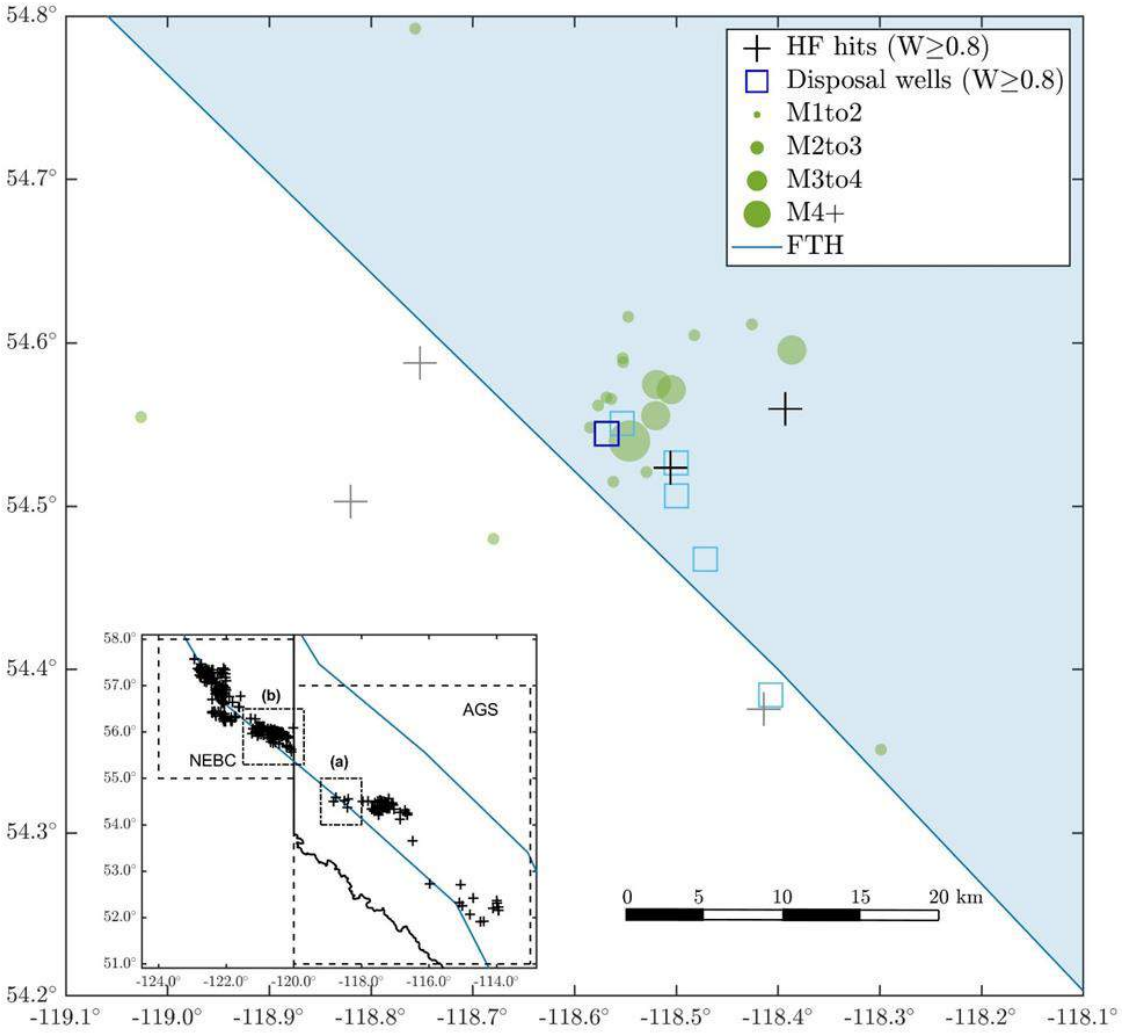

*Figure 8 – Zoom of area in AGS catalogue for which a cluster of events is potentially associated with both disposal wells (squares) and HF wells (squares). The range of W values for the plotted HF wells is 0.55 to 1.0, with HF wells with W≥0.8 indicated by darker shade. The range of Ww values for the plotted disposal wells is 0.20 to 0.84, with Ww≥0.8 indicated by darker shade. All catalogue events of **M**≥1 (2014-2019) are shown. Inset boxes highlight location.*

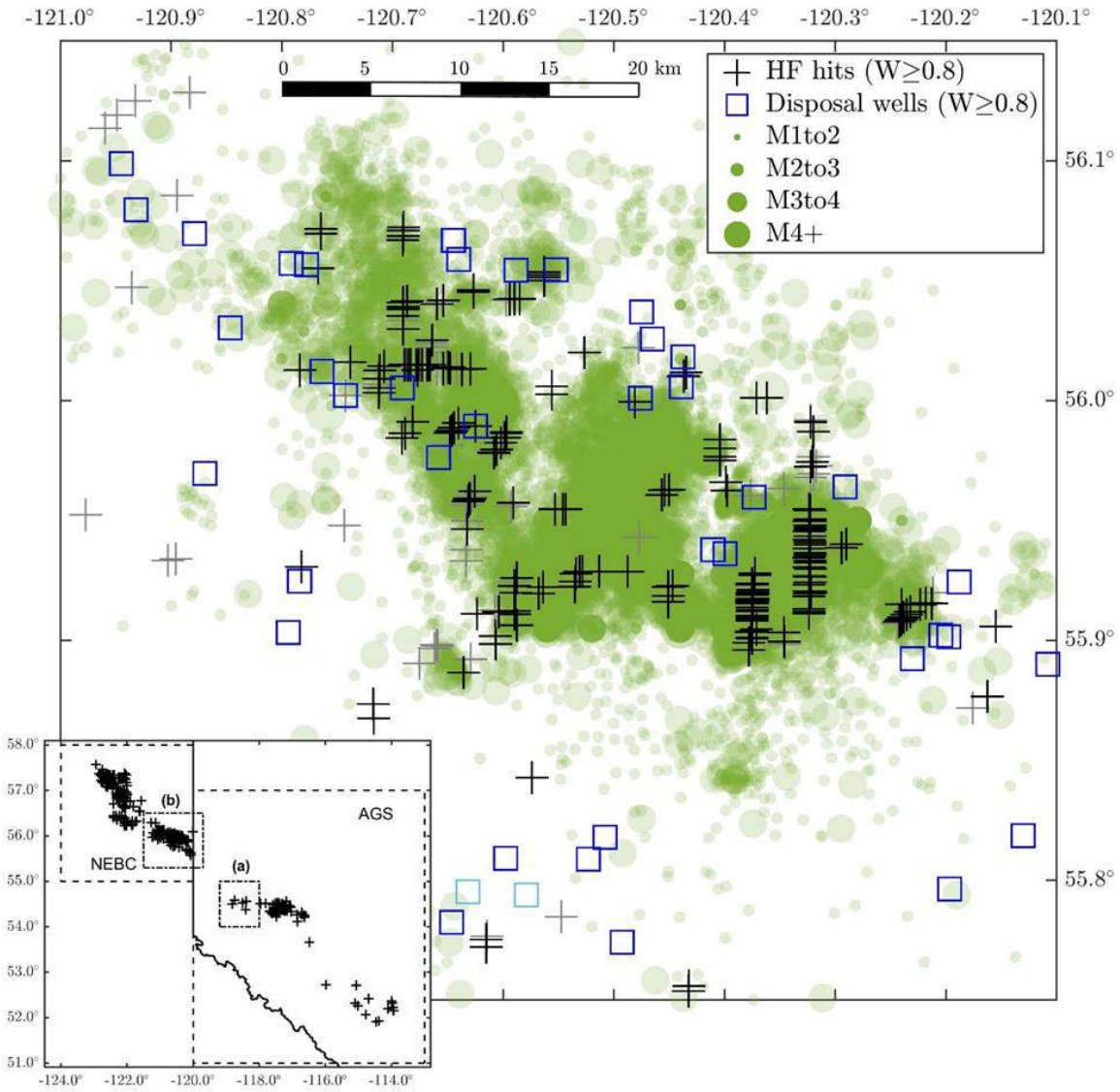

*Figure 9 – Zoom of area in NEBC catalogue for which a cluster of events is potentially associated with both disposal wells (squares) and HF wells (squares). The range of W values for the plotted HF wells is 0.35 to 1.0, with HF wells with W≥0.8 indicated by darker shade. The range of Ww values for the plotted disposal wells is 0.40 to 1.0, with Ww≥0.8 indicated by darker shade. All catalogue events of **M**≥1 (2014-2019) are shown. Inset boxes highlight location.*

Comparison of Inferred Activation Rates with Regional Seismicity and Well Statistics

We check whether our overall induced seismicity rates are consistent with observed seismicity and assess how much induced seismicity is likely due to disposal wells versus HF wells. To do this, we use the AGS catalog for all years from 2006-2020 to track seismicity rates and compare to HF well rates. This exercise is performed only for the AGS catalogue (51 to 57N and east of 119; the area shown on Figure 1). The reason is that the NEBC catalogue is much shorter in time span, covering only the period from 2014 to 2019. An examination of magnitude-recurrence

statistics suggests that the AGS catalogue for the selected time and space window is complete from at least **M**2.5 (see also Cui et al., 2016). We count the number of **M**≥2.5 and **M**≥3 events per annum (p.a.) from 2006 and compare it to the total number of HF and disposal wells, as shown in Figure 10. To make the rates for **M**≥2.5 and **M**≥3 easier to compare, we divide the p.a. rates for **M**≥2.5 by 3 to convert them to the equivalent rates for **M**≥3, assuming a Gutenberg-Richter relation with a slope of 1. We observe that there were 2 to 3 **M**≥3 events p.a. until 2011, when HF wells started to become numerous. Since 2012, there have been ~10 events of **M**≥3 p.a., which are potentially associated with ~1500 to 2000 HF wells p.a. The number of disposal wells has been relatively constant (~1500), suggesting that the disposal wells are associated with, at most, 2 to 3 **M**≥3 events p.a. (assuming that the contributions from natural events are negligible; see next section). We thus infer from Figure 10 that up to 80% of the observed seismicity in Alberta is in response to the increase in HF wells. By comparison, in Table 1, we identify 50% to 60% of seismicity in Alberta as being associated with HF wells (70% for NEBC). The figures in Table 1 are consistent with a previous study by Atkinson et al. (2016), who concluded that ~60% of seismicity in the WCSB is associated with HF wells. The inference is that about 20% of the seismicity occurs along with the rise of HF wells but may not be a direct response.

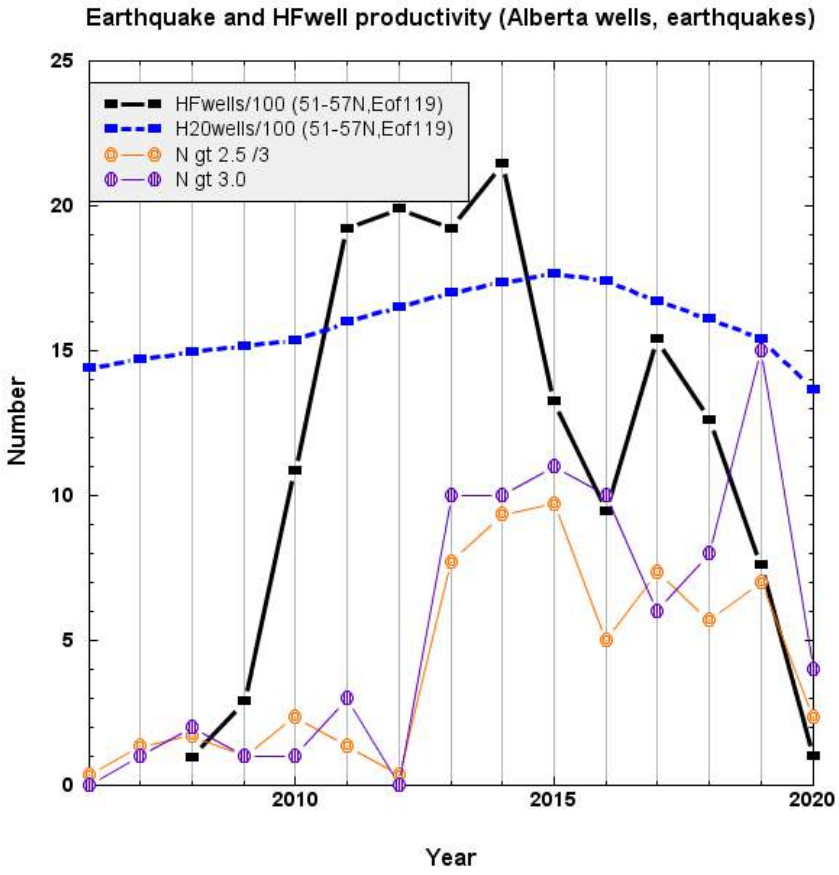

Figure 10. Yearly counts of earthquakes and HF wells in area 51-57N, east of 119W. HF well count is divided by 100. Disposal wells counts (divided by 100) in each year also shown. Count

*of **M**≥2.5 is divided by 3 (to be equivalent to rate for **M**≥3, for assumed Gutenberg-Richter slope of 1). HF wells database for 2020 is incomplete.*

An interesting observation on Figure 10 is that there appears to be a lag of ~2 years between the increase of HF wells and the increased seismicity. Most of the events are coming from the Fox Creek area, where abundant seismicity has been associated largely with Duvernay operations. Even though HF wells became widespread in the area starting in 2011, it was not until 2013 (after ~1000 HF wells) that the area became active. However, once the area became active, it has stayed active. This may reflect some cumulative effects, in which it is easier to retrigger seismicity once triggered (Bao and Eaton, 2016; Chapman, 2021). On the other hand, lags of up to 5 years have been noted in the onset of seismicity related to gas production (Baranova et al., 1999) – it may be that some of the increased activity is related to increased production – and thus related to HF wells only indirectly (*i.e.* production follows HF operations). This could account for the missing 20% of seismicity (*i.e.* if 80% of the seismicity is in response to HF wells, but only 60% is directly related in terms of timing). We may also infer from Figure 10 that the presence of a disposal well near an HF hit does not necessarily mean the HF well was not involved. The HF wells are clearly generating more seismicity than are the disposal wells (by a ratio of ~5:1). Moreover, since the time lag is short for flagging HF wells, the event is most likely related to the HF well (at least in part), unless the disposal well is regularly generating seismicity over its operational period.

Subdivision of W Scores into Contributing Components

We observe on Figure 10 that the rate of seismicity is relatively constant in the period 2013-2019. The sum of the **M**≥3 events over this 7-year period is the total seismicity rate, N3sum. This can be broken down into a sum from natural (N3nat), HF (N3hf), and disposal (N3d): N3sum=N3nat + N3hf + N3d. The natural earthquake contribution can be calculated from the earthquake recurrence parameters of Halchuk et al. (2014) for the FTH zone (Figure 1), because they assessed these rates using seismicity to 2010, after deleting the most prolific known induced seismicity clusters. The area of HF wells lies almost entirely within FTH. The number of natural earthquakes p.a. in the portion of FTH considered in our study within the AGS catalogue (i.e. east of 119; shaded area in Figure 1) can be calculated based on its percentage of the total FTH area, using the magnitude recurrence relation of Halchuk et al. (2014). By inspection, the oil and gas region in the AGS catalogue accounts for ~55% of the FTH area. Accordingly, we calculate that Halchuk et al.'s rate of 0.68 **M**≥3 for the whole FTH represents a rate of ~0.37 **M**≥3 for the portion of FTH used in our AGS study catalogue. This is the natural seismicity rate. It follows from inspection of Figure 10 that we have observed ~8 events of **M**≥3 p.a. from HF wells and ~2 events p.a. from disposal wells. We would therefore expect the sum of W from events associated with HF wells to be ~8 p.a. at the **M**3 level, or ~80 p.a. at the **M**2 level (assuming a Gutenberg-Richter slope of 1), for the AGS catalogue. Based on the statistics in Table 1, we have a sum of W=239 for the 2014-2019 period (counting all events, with W:max=1), or Wsum=40 p.a (=239/6yrs). Thus, the number of potentially associated **M**≥2 events in our study may be an underestimate; alternatively, it may reflect that our associations do not include indirect contributions following HF wells (re-triggering; production, etc.). This overall check of our estimated rates against the observed seismicity patterns provides further confidence that we are not overcounting the number of earthquakes associated with HF wells.

Effect of formation depth on association potential

Recent studies have begun to quantify the relationship between the activation potential of HF wells and the depth of operations. For example, Ries et al. (2020) showed that likelihood of induced seismicity in a susceptible area of Oklahoma increased with the depth of the HF well, from ~5% for wells at 1.5 km depth, to ~50% for wells at 5.5 km. GA20 reported that the association rate between **M**≥3 earthquakes and HF wells varied with formation across the WCSB, from <0.1% per well for Cardium HF wells (shallow) to >6% for Duvernay HF wells (deep).

Figure 11 breaks down the contributions of the W scores for HF wells by formation depth, for both the AGS and NEBC catalogues. To prepare this figure, we organize the W scores by well, listing all wells flagged with W≥0.35. For each such well, we assign the W score of the highest-scoring event. Thus each well is considered only once, but an event may be considered more than once. This will result in an overcount, as per Table 1, by a factor of 2.09 for the AGS catalogue or 2.23 for the NEBC catalogue. We sort the wells by depth (in bins of 0.5 km) and age (Cretaceous, Triassic, Paleozoic). We sum within these groups, in each case dividing the sum by the corresponding overcount factors. To express these scores as a per-well likelihood of seismicity at the **M**>2 level, we divide the adjusted W sum within each bin by the total number of HF wells within the bin.

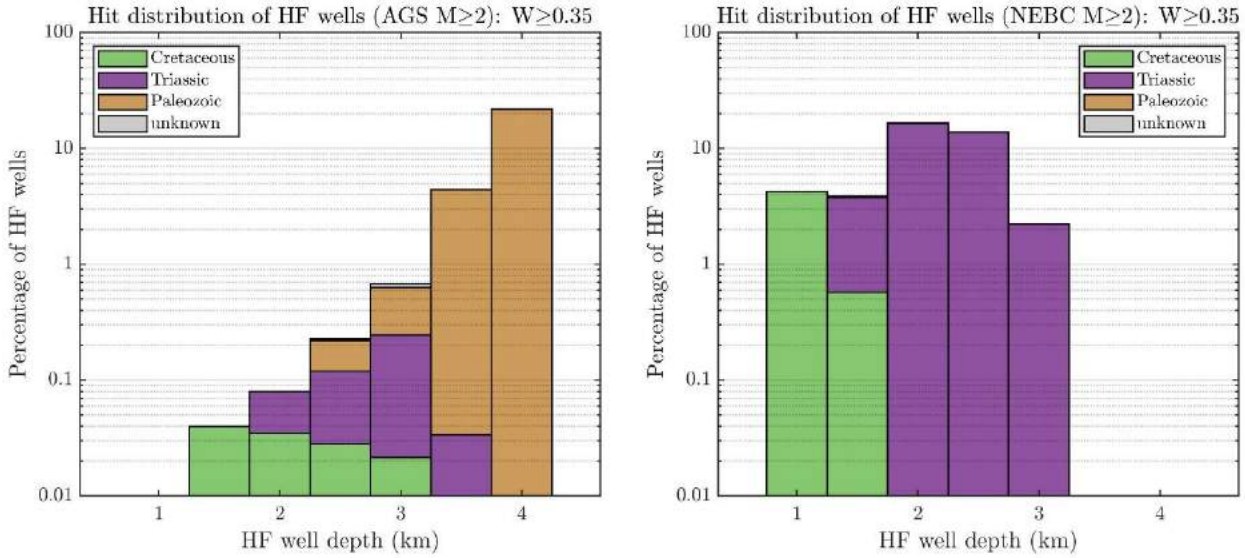

*Figure 11. Percentage of HF wells associated with **M**≥2 seismicity as a function of HF well depth, for AGS and NEBC catalogues, based on summing W scores in depth bins, and dividing by overcount factor. Shading shows formation age (Paleozoic, Triassic, and Cretaceous).*

The likelihood of induced seismicity at the **M**≥2 level increases with depth in central Alberta, from ~0.04% per well for very shallow wells (1.5 km) to >20% for deep wells (4 km). There is also an apparent correlation with formation age, with Cretaceous wells having a much lower likelihood of association than Triassic or Paleozoic wells. The depth and age factors are not independent, as the deeper wells are also the older wells. Depth may be related to susceptibility

due to increasing pressure; age may play a factor due to increasing fault density and maturity and other geologic factors (e.g. Schultz et al., 2020a).

In NEBC, the relationship of the percentage of HF wells associated with seismicity with depth and age is different. There is no apparent relationship with depth, but some relationship with age, with most of the well hits being for Triassic formations (in particular, the Montney). However, because there are no deep Paleozoic wells, the differences may not be as profound as they appear. NEBC is more highly susceptible to HF seismicity than is Alberta; the association percentages are higher in the sampled depths (<3.5 km) and ages (Cretaceous, Triassic) by factors of 2 to >10 in comparison to the corresponding rates in central Alberta.

The utility of the plot of W versus depth is in expressing the relative likelihood by depth and formation age. It may be noted that the peaks of the distribution correspond to the formations most associated with HF induced seismicity. The Montney formation is largely responsible for the high association rates at formation depths near 2 to 3 km, whereas the Duvernay formation is largely responsible for the high association rates at greater depth . If we consider the breakdown of HF well activity shown on Figure 10 by formation age, in Alberta ~ 0.12% of Cretaceous wells, 0.39% of Triassic and 26.6% of Paleozoic HF wells are associated with **M**≥2 seismicity. In NEBC the corresponding percentages are 4.8% and 35.5%, for Cretaceous and Triassic wells, respectively. Though broken down differently, this is in qualitative agreement with the findings of GA20, who reported that susceptibility varied by formation from <0.1% for the Cardium (Cretaceous) to ~6% for the Duvernay (Paleozoic).

In addition to the relationship between activation potential and formation age, there is also a relationship between age and event productivity. This is expected because the resource plays in the Triassic and Montney formations tend to use much larger injected volumes, and event productivity tends to scale with volume (Schultz et al., 2018). The average number of **M**≥2 events per potentially associated HF wells in Alberta (*i.e.* the expected number of events, conditioned on the activation of the well, using the highest-scoring well for each event) is 1.1 for Cretaceous wells, 1.9 for Triassic wells and 2.9 for Paleozoic wells. In NEBC, the average number of **M**≥2 events per potentially associated HF well is 6 for Cretaceous and 7.9 for Triassic wells. In Alberta, the most prolific sequences have been in the Duvernay formation, whereas in NEBC, the most prolific sequences have been in the Montney formation. The low seismic productivity of HF wells in many formations, combined with their low activation potential, explains the relative lack of documented induced events in such formations. A significant event associated with HF wells is expected to be a rare event, except within the highly susceptible Duvernay and Montney formations.

In the areas in which disposal wells may play a significant role in triggering seismicity (e.g. as shown in Fig. 8, 9), the candidate disposal wells with the highest Ww scores range in depth from ~2100 to 4500 m in Alberta, or ~900 to ~2700m in NEBC. The corresponding ages of the formations are mostly Paleozoic in Alberta (including the well in Fig. 8 with Ww>0.8), and mostly Cretaceous in NEBC (including those with Ww>0.8 in Fig. 9).

Conclusions

We have updated the results of GA20 on the relationship between seismicity and HF wells using a refined *W* metric as applied to improved regional catalogues. The *W* metric is a simple measure of the relative strength of spatiotemporal association. It is not a formal likelihood or

probability. However, it could carry such implications if used within a probabilistic hazard analysis framework. For example, the *W* metric could be used to assess the likelihood that a future HF operation may trigger seismicity within a certain time and distance range (e.g. Atkinson, 2017); this would be akin to a prior probability in a Bayesian sense.

Using the *W* metric, we assess the average regional rate of association of HF wells with **M**≥2 seismicity, from 2014-2019, to be ~0.9% per well in central Alberta, and ~16% per well in NEBC (areas on Figures 1, 2). Overall, this represents ~50% of all observed **M**≥2 seismicity in Alberta, and ~70% in NEBC (see Table 1). The possibility that contributions from disposal wells have inflated the HF rates is low in Alberta, with only ~2% of the HF hits also having a strong association to nearby disposal wells. In NEBC, ~25% of the HF hits also have a strong association to disposal wells, so it is possible that NEBC HF rates may be overestimated.

Our updated results are generally consistent with our previous studies, including those of Atkinson et al. (2016) and GA20, who reported that ~60% of observed seismicity appeared to be associated with HF wells. Our results are also in agreement with Chapman (2021), who concluded that ~70% of **M**≥3 seismicity in NEBC is associated with HF wells. Chapman obtained a per well association rate for **M**≥3 seismicity of 1.7% for the Montney region, using a different catalogue and tighter distance criteria (5km); he noted that this calculated rate was considered to be a low estimate due to 8 excluded **M**≥3 events that appeared to be triggered events, but were located >5 km from the well. In comparison, if we consider just **M**≥3 events using our new criteria, we infer a per well activation rate of 4% in NEBC (or 0.2% in Alberta). The relative consistency of findings across studies that utilized evolving methodologies and datasets provides confidence that the results are robust, in the regional average context in which they are intended.

The induced seismicity potential is markedly higher in NEBC in comparison to Alberta. Within each region, the activation rates and event rates vary greatly with formation depth and age. In Alberta, there is a clear trend to increasing activation potential with depth and age, in agreement with previous studies (e.g. see Schultz et al., 2020; Reis et al., 2020). In NEBC, the trend is less clear, though this may be largely attributed to the lack of HF wells in deeper and older formations.

Data and Resources

The database of ~700,000 wells (all types) was searched using geoSCOUT software (geoLOGIC systems Ltd.) licensed to Western University. The AGS catalogue is obtained from Alberta Geological Survey Earthquake Dashboard at https://ags-aer.shinyapps.io/Seismicity_waveform_app/ (last accessed January 2021). The Visser et al. (2018, 2019) catalogue for northeastern B.C. (NEBC catalogue) is obtained from: Geological Survey of Canada, Open File 8335, 2017, 28 pages, https://doi.org/10.4095/306292 (Open Access); the 2019 additions to the Visser et al. catalogue were provided by A. Mahani (pers. Comm., Sept., 2020). The Composite Seismicity Catalogue for Alberta and British Columbia is available at www.inducedseismicity.ca (last accessed January 2021). Honn Kao (pers. comm., Sept. 2020) kindly provided the CMT solution database. The Nanometrics catalogue (for TransAlta) was provided to Western University by Nanometrics and TransAlta (private Athena website, last accessed Jan., 2021).

Acknowledgements

We are grateful to Rob Skoumal, whose comments during the review of GA20 prompted us to examine whether there was a better way to define the time lag metric. We thank Ali Mahani for making available the Visser et al. catalogue for 2019 in advance of publication.

References

Atkinson, G. M., Eaton, D. W., Ghofrani, H., Walker, D., Cheadle, B., Schultz, R., Shcherbakov, R., Tiampo, K. F., Gu, J., Harrington, R. M., Liu, Y., van der Baan, M., & Kao, H. (2016). Hydraulic fracturing and seismicity in the Western Canada Sedimentary Basin. Seismological Research Letters, 87(3), 631-647. https://doi.org/10.1785/0220150263.

Atkinson, G. M. (2017). Strategies to prevent damage to critical infrastructure due to induced seismicity. FACETS, 2, 374-394. https://doi.org/10.1139/facets-2017-0013.

Atkinson, G. M., Eaton, D. W., & Igonin, N. (2020). Developments in understanding seismicity triggered by hydraulic fracturing. Nature Reviews Earth & Environment, 1, 264-277, https://doi.org/10.1038/s43017-020-0049-7.

Chapman, A. (2021). Hydraulic Fracturing, Cumulative Development and Earthquakes in the Peace River Region of British Columbia, Canada. Journal of Geoscience and Environment Protection, **9**, 55-82. https://doi.org/10.4236/gep.2021.95006.

Cui, L., and G. M. Atkinson (2016), Spatiotemporal variations in the completeness magnitude of the Composite Alberta Seismicity Catalog (CASC), Seismol. Res. Lett., 87(4), 853-863, https://doi.org/10.1785/0220150268.

Dokht, R. M. H., Smith, B., Kao, H., Visser, R., and Hutchinson, J. (2020). Reactivation of an intraplate fault by mine-blasting events: Implications to regional seismic hazard in Western Canada. Journal of Geophysical Research: Solid Earth, 125(6), e2020JB019933. https://doi.org/10.1029/2020JB019933

Eaton, D. W., and Schultz, R., (2018). Increased likelihood of induced seismicity in highly over-pressured shale formations, Geophysical Journal International, 214(1), 751-757, https://doi.org/10.1093/gji/ggy167.

Ellsworth, W. L. (2013), Injection-induced earthquakes, Science, 341(6142), 1225942, https://doi.org/10.1126/science.1225942.

Ghofrani, H., and Atkinson, G. M. (2016). A preliminary statistical model for hydraulic fracture-induced seismicity in the Western Canada Sedimentary Basin, Geophys. Res. Lett., 43(19), 10,164-10,172, https://doi.org/10.1002/2016GL070042.

Ghofrani, H., and G. M. Atkinson (2020). Activation Rate of Seismicity for Hydraulic Fracture Wells in the Western Canada Sedimentary Basin. Bulletin of the Seismological Society of America, 110(5), 2252-2271. doi: https://doi.org/10.1785/0120200002.

Ghofrani, H. and G. M. Atkinson (2021). Reply to Comment on "Activation rate of seismicity for hydraulic fracture wells in the Western Canadian Sedimentary Basin by Ghofrani and Atkinson (2020)" by James P. Verdon, and Julian J. Bommer.

Gu Y.J., Okeler A., Shen L., and Contenti S. (2011). The Canadian Rockies and Alberta Network (CRANE): New Constraints on the Rockies and Western Canada Sedimentary Basin. Seismological Research Letters; 82(4), 575-588. doi: https://doi.org/10.1785/gssrl.82.4.575

Halchuk S. C. Adams J. E., and Allen T. I. (2015). Fifth generation seismic hazard model for Canada: Grid values of mean hazard to be used with the 2015 National Building Code of Canada, Geol. Surv. Canada Open-File Rept. 7893, 26 pp., https://doi-org.proxy1.lib.uwo.ca/10.4095/297378.

Holmgren, J. M., Atkinson, G. M., Ghofrani, H. (2019). Stress Drops and Directivity of Induced Earthquakes in the Western Canada Sedimentary Basin. Bull. Seismol. Soc. Am. 109(5), 1635-1652. https://doi.org/10.1785/0120190035.

Holmgren, J. M., Atkinson, G. M., Ghofrani, H. (2020). Reconciling Ground Motions and Stress Drops for Induced Earthquakes in the Western Canada Sedimentary Basin. Bull. Seismol. Soc. Am. 110(5), 2398-2410. https://doi.org/10.1785/0120190308.

Hutton, L. K., and Boore, D. M., (1987). The ML scale in Southern California. Bull. Seismol. Soc. Am. 77(6), 2074-2094.

Kolaj et al. (2020). Sixth Generation Seismic Hazard Model of Canada: input files to produce values proposed for the 2020 National Building Code of Canada. Geological Survey of Canada, Open File 8630, 2020, 15 pages, https://doi.org/10.4095/327322.

Kozłowska, M., Brudzinski, M. R., Friberg, P., Skoumal, R. J., Baxter, N. D., and Currie, B. S., (2018). Proceedings of the National Academy of Sciences, 115(8) E1720-E1729, https://doi.org/10.1073/pnas.1715284115.

Lomax, A., J. Virieux, P. Volant and C. Berge, 2000. Probabilistic earthquake location in 3D and layered models: Introduction of a Metropolis-Gibbs method and comparison with linear locations, in Advances in Seismic Event Location Thurber, C.H., and N. Rabinowitz (eds.), Kluwer, Amsterdam, 101-134.

Pawley, S., Schultz, R., Playter, T., Corlett, H., Shipman, T., Lyster, S., & Hauck, T. (2018). The geological susceptibility of induced earthquakes in the Duvernay play. Geophysical Research Letters, 45(4), 1786-1793. https://doi.org/10.1002/2017GL076100.

Ries, R., Brudzinski, M. R., Skoumal, R. J., and Currie, B. S., (2020). Factors Influencing the Probability of Hydraulic Fracturing-Induced Seismicity in Oklahoma. Bulletin of the Seismological Society of America, 110(5), 2272-2282. doi: https://doi.org/10.1785/0120200105.

Germán Rodríguez-Pradilla, David W. Eaton (2020). Automated Microseismic Processing and Integrated Interpretation of Induced Seismicity during a Multistage Hydraulic-Fracturing Stimulation, Alberta, Canada. Bulletin of the Seismological Society of America, 110(5), 2018-2030. doi: https://doi.org/10.1785/0120200082.

Rubinstein, J., and A. Babaie Mahani (2015), Myths and facts on wastewater injection, hydraulic fracturing, enhanced oil recovery, and induced seismicity, Seismol. Res. Lett., 86(4), 1060-1067, https://doi.org/10.1785/0220150067.

Schultz, R., Mei, S., Pană, D., Stern, V., Gu, Y. J., Kim, A., & Eaton, D. (2015). The Cardston earthquake swarm and hydraulic fracturing of the Exshaw Formation (Alberta Bakken play). Bulletin of the Seismological Society of America, 105(6), 2871-2884. https://doi.org/10.1785/0120150131.

Schultz, R., Stern, V., Novakovic, M., Atkinson, G., and Gu, Y. J. (2015). Hydraulic fracturing and the Crooked Lake Sequences: Insights gleaned from regional seismic networks. Geophysical Research Letters, 42, 2750-2758. https://doi.org/10.1002/2015GL063455.

Schultz, R., Corlett, H., Haug, K., Kocon, K., MacCormack, K., Stern, V., Shipman, T., (2016). Linking fossil reefs with earthquakes: geologic insight to where induced seismicity occurs in Alberta. Geophys. Res. Lett. 43(6), 2534-2542. https://doi.org/10.1002/2015GL067514.

Schultz, R., Wang, R., Gu, Y. J., Haug, K., and Atkinson, G. (2017). A seismological overview of the induced earthquakes in the Duvernay play near Fox Creek, Alberta. Journal of Geophysical Research: Solid Earth, 122(1), 492-505. https://doi.org/10.1002/2016JB013570.

Schultz, R., Skoumal, R. J., Brudzinski, M. R., Eaton, D., Baptie, B., and Ellsworth, W. (2020a). Hydraulic fracturing-induced seismicity. Reviews of Geophysics, 58(3), e2019RG000695. https://doi.org/10.1029/2019RG000695.

Schultz R, Beroza G, Ellsworth W, Baker J (2020b). Risk-informed recommendations for managing hydraulic fracturing–induced seismicity via traffic light protocols. Bulletin of the Seismological Society of America, 110(5), 2411-2422, doi: https://doi.org/10.1785/0120200016.

Stern V.H., Schultz R.J., Shen L., Gu Y.J., and Eaton D.W. (2013). Alberta Earthquake Catalogue, Version 1.0: September 2006 through December 2010. AER/AGS Open File Report 2013-15 (https://www.ags.aer.ca/document/OFR/OFR_2013_15.pdf)

Verdon and Bommer (2021). Comment on "Activation rate of seismicity for hydraulic fracture wells in the Western Canadian Sedimentary Basin" by Ghofrani and Atkinson (2020).

Visser, R., Smith, B., Kao, H., Babaie Mahani, A., Hutchinson, J., & McKay, J. E. (2017). A comprehensive earthquake catalogue for northeastern British Columbia and western Alberta, 2014-2016. Geological Survey of Canada Open-File Report, 8335, 27. https://doi.org/10.4095/306292.

Visser, R, Kao, H, Smith, B, Goerzen, C, Kontou, B, Dokht, R M H, Hutchinson, J, Tan, F, and Babaie Mahani (2020). A comprehensive earthquake catalogue for the Fort St. John-Dawson Creek region, British Columbia, 2017-2018, A. Geological Survey of Canada, Open File 8718, 2020, 28 pages, https://doi.org/10.4095/326015 (Open Access).

Wang, R., Gu, Y. J., Schultz, R., and Chen, Y. (2018). Faults and non-double-couple components for induced earthquakes. Geophysical Research Letters, 45, 8966-8975. https://doi.org/10.1029/2018GL079027

Wang, J., Li, T., Gu, Y. J., Schultz, R., Yusifbayov, J., & Zhang, M. (2020). Sequential fault reactivation and secondary triggering in the March 2019 Red Deer induced earthquake

swarm. Geophysical Research Letters, 47(22), e2020GL090219. https://doi.org/10.1029/2020GL090219.

Yenier, E. (2017). A Local Magnitude Relation for Earthquakes in the Western Canada Sedimentary Basin, Bull. Seismol. Soc. Am. 107(3), 1421-1431, https://doi.org/10.1785/0120160275.

Zhang, H., Eaton, D. W., Li, G., Liu, Y., and Harrington, R. M. (2016). Discriminating induced seismicity from natural earthquakes using moment tensors and source spectra. Journal of Geophysical Research: Solid Earth, 121, 972-993. https://doi.org/10.1002/2015JB012603